

# Thermal Kinetics of Gold Nanosphere under a Burst of Femtosecond Laser †

Selma Mediene \*  and Assia Rachida Senoudi

Physics Department, Theoretical Physics Laboratory, Tlemcen University, Tlemcen 13000, Algeria; arsenoudi@gmail.com

\* Correspondence: selma.mediene@univ-tlemcen.dz or selmamediene@gmail.com

† Presented at the 4th International Online Conference on Nanomaterials, 5–19 May 2023; Available online: <https://iocn2023.sciforum.net>.

**Abstract:** The thermal dynamics of a spherical gold nanoparticle under a femtosecond laser burst irradiation at 550 nm wavelength, 100-fs pulse duration, and  $F = 1 \text{ J/m}^2$  laser fluence are investigated numerically. A unique spherical gold nanoparticle immersed in water is heated by a single pulse laser and then after by a number of sub-pulses. The two-temperature model is used to describe the energy-exchange dynamics of the gold nanoparticle, in addition to Fourier's law and to the relationship between the thermal conductivity of the water and the temperature. Our results show that the irradiation of a gold nanoparticle by a femtosecond laser burst, with a separation time between sub-pulses less than the thermal relaxation time, leads to a fast heat accumulation which enhances the temperatures of the electron, the phonon, and the water near the gold nanoparticle's surface.

**Keywords:** femtosecond laser; gold nanoparticle; thermal accumulation; two-temperature model

## 1. Introduction

The interaction between metallic nanoparticles with intense light fields is an appealing field of science. In particular, gold nanoparticles (AuNps)—because of their potential applications in nonlinear optics [1], solar energy [2] chemical sensing [3] and in nano-medicine, spherical AuNps—are widely used for photothermal drug delivery or in hyperthermia cancer therapy [4,5] due to their relative ease of fabrication, non-toxicity, ease of binding to antibodies, and due to their excellent thermal, optical, chemical, and biological properties. These unique and amazing properties are due to the localized surface plasmon resonance effect (LSPR), defined by collective oscillations of free electrons at the AuNp surface when irradiated by a laser field at a specific wavelength. AuNps are characterized by their high absorption cross-section and neglected scattering [6] at visible or infrared frequencies (depending on the size and the shape of the AuNp). Optical cross-sections can be calculated according to the Mie diffusion theory for the spherical shape [7]. The computer calculation of optical cross-sections of AuNp can be performed using a FORTRAN code [8].

In hyperthermia, free electrons absorb the laser energy due to the inverse bremsstrahlung; they are relaxed through electron–electron scattering over a time of 100 fs up to 1 ps, and then the lattice starts to heat up as a result of electron–phonon scattering until its thermal equilibrium is reached after several tens of ps. Then, the heat is transferred from particle into the surrounding medium through phonon–phonon coupling in a few ns [9], meaning the thermalization phase is very short. The electron and the lattice subsystems can be characterized by their temperatures ( $T_e$ ,  $T_L$ ), which are computed using the two-temperature diffusion model (TTM) [10–15]. In the TTM, we included the energy dissipation due to the heat conduction through the AuNp/water interface. The deposition of radiation energy is generally non-uniform throughout the particle volume; however, for the case where  $2\pi R/\lambda < 1$  ( $R$  is the radius of the AuNp and  $\lambda$  is the wavelength of incident light), we assumed that the laser energy deposited on the AuNp is uniform throughout its volume [13],



**Citation:** Mediene, S.; Senoudi, A.R. Thermal Kinetics of Gold Nanosphere under a Burst of Femtosecond Laser. *Mater. Proc.* **2023**, *14*, 37. <https://doi.org/10.3390/IOCN2023-14511>

Academic Editor: Wolfgang Heiss

Published: 5 May 2023



**Copyright:** © 2023 by the authors. Licensee MDPI, Basel, Switzerland. This article is an open access article distributed under the terms and conditions of the Creative Commons Attribution (CC BY) license (<https://creativecommons.org/licenses/by/4.0/>).

and this simplified the problem where the temperatures were expressed only in relation to time.

In this work, we performed numerical simulations to study the heat accumulation due to a femtosecond laser burst. Single 40 nm diameter spherical AuNp, immersed in water, is heated first by one single Gaussian 100 fs pulse and  $F = 1 \text{ J/m}^2$  laser fluence (fixed in the numerical simulation), and then after by a sequence of sub-pulses having different separation times. The separation times are modified for studying the heat accumulation in the AuNp. We computed the temporal evolution of the electron gas, the gold lattice, and the water near the AuNp surface temperatures, both for one pulse and for five sub-pulses per burst. The obtained results show that the irradiation of the AuNp by a femtosecond laser burst, with a separation time less than the thermal relaxation time, enhances the electron, phonon, and AuNp/water interface temperatures without increasing the laser energy.

## 2. Materials and Methods

The TTM as shown in Equation (1) is composed of two equations; the first one describes the thermal energy transfer from the electron gas to the lattice and the second one describes the transfer from the lattice to the surrounding water:

$$\begin{cases} C_e \frac{dT_e(t)}{dt} = -g(T_e(t) - T_L(t)) + S(t) \\ C_L \frac{dT_L(t)}{dt} = g(T_e(t) - T_L(t)) - Q_C \end{cases} \quad (1)$$

$T$  is the temperature, and  $C$  is the heat capacity per unit of volume which depends on  $T$ , where  $e$  and  $L$  denote the electron and lattice, respectively;  $S(t)$  represents the laser energy deposition into the electron subsystem of the AuNp per unit of time ( $t$ ) and per unit of volume; the electron–phonon coupling factor  $g$  describes the energy exchange from the electrons to the lattice through electron–phonon scattering and it can be expressed [10] by  $g = g_0 (A_e/B_L(T_e + T_L) + 1)$  with  $g_0 = 2.2 \times 10^{16} \text{ Wm}^{-3} \text{ K}^{-1}$ , and the coupling factors at room temperature,  $A_e = 1.2 \times 10^7 \text{ K}^{-2} \text{ s}^{-1}$  and  $B_L = 1.23 \times 10^{11} \text{ K}^{-1} \text{ s}^{-1}$ , being material constants. Table 1 summarizes the specific values of the thermophysical properties used in this paper.

**Table 1.** Parameters used in numerical computation.

Parameter	Value	Ref.
AuNp		
Electron heat capacity, $C_e$ ( $\text{Jm}^{-3} \text{ K}^{-1}$ )	$C_e = 70 \times T_e$	[12]
Lattice heat capacity, $C_L$ ( $\text{Jm}^{-3} \text{ K}^{-1}$ )	$C_L = \rho_{gold} \times (109.707T_L - 3.4 \times 10^{-4}T_L^2 + 5.24 \times 10^{-7}T_L^3 - 3.93 \times 10^{-10}T_L^4 + 1.17 \times 10^{-13}T_L^5)$	[11]
Density, $\rho_{gold}$ ( $\text{Kg m}^{-3}$ )	$\rho_{gold} = 1.93 \times 10^4$	[12]
Gold melting temperature, $T_m$ (K)	1337	[5,11]
Water		
Critical temperature, $T_{Cr}$ (K)	647	[5,11]
Boiling temperature, $T_b$ (K)	3130	[5,11]
Cavitation threshold $T_{cav}$ (K)	573	
Thermal conductance at the gold/water interface, $G$ ( $\text{Wm}^{-2} \text{ K}^{-1}$ )	$G = 105 \times 10^6$	[5]
Thermal conductivity, $k_\infty$ at $T = 300 \text{ K}$ ( $\text{Wm}^{-1} \text{ K}^{-1}$ )	0.61	[5]

The expression of  $S(t)$  [14] is given as follows:

$$S(t) = \frac{C_{abs} \times P(t)}{V_p} \quad (2)$$

$C_{abs}$  is the optical absorption efficiency,  $V_p$  is the AuNp volume, and  $P(t)$  is the intensity of the pulsed laser.

Equation (3) describes  $P(t)$  having a Gaussian distribution, for multi-pulse irradiation [14], with  $N$  being the number of sub-pulses per burst,  $t_{sep}$  being the separation time between two consecutive sub-pulses,  $F$  being the laser fluence, and  $\tau_p$  being the pulse duration.

$$P(t) = \sum_{j=1}^N \frac{2\sqrt{\ln 2}}{\sqrt{\pi}} \frac{F}{\tau_p} \exp\left(-4\ln 2(t - 2\tau_p - (j-1)t_{sep})^2 / \tau_p^2\right) \quad (3)$$

In Equation (1), the rate of the heat conduction loss from the AuNp to its surroundings per unit of volume ( $Q_C$ ) can be computed according to Fourier's law [13] as:

$$Q_C = \frac{S_p}{R} \int_{T_\infty}^{T_s} k(T) dT \quad (4)$$

$T_s$  is the temperature at the AuNp/water interface,  $k(T)$  is the thermal conductivity of the water, and  $S_p$  is the surface area of the spherical AuNp. The dependence of the thermal conductivity of the external medium temperature is given as a power law temperature function:  $k(T) = k_\infty(T/T_\infty)^b$  in which  $k_\infty$  represents the thermal conductivity of the surrounding medium at  $T_\infty = 300$  K. For water, the parameter  $b = 1$ , as reported in [13]. The integration of Equation (4) leads to

$$Q_C = 2\pi R k_\infty T_\infty \left( \left( \frac{T_L(t)}{T_\infty} \right)^2 - 1 \right) \quad (5)$$

The temperature at the AuNp/water interface  $T_{ws}$  [10] can be expressed as

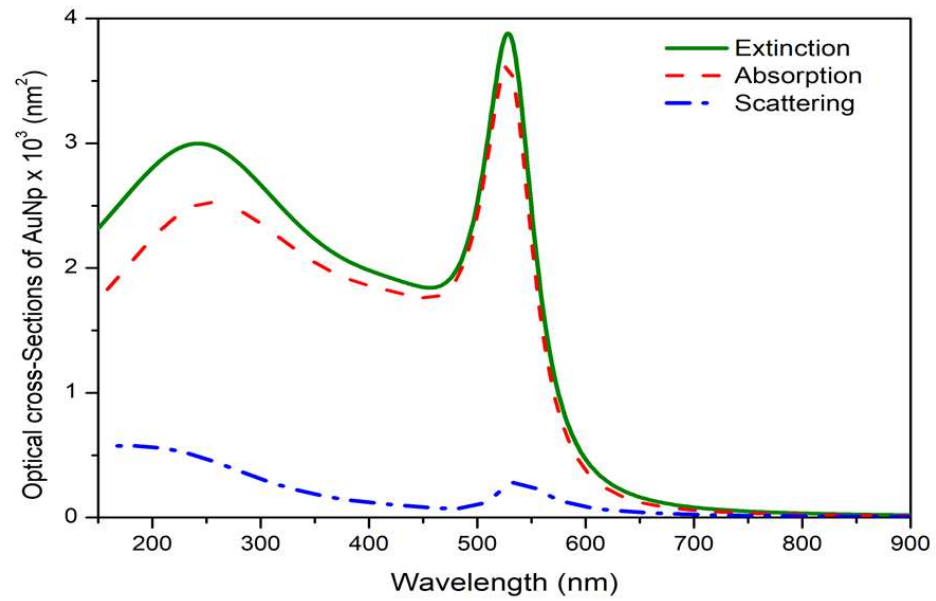
$$T_{ws}(t) = T_L(t) - \frac{Q_C}{G S_p} \quad (6)$$

$G$  is the interface thermal conductivity that describes the energy transfer from the particle to the water. Phase transitions are not included in the model because of the low value chosen for the fluence laser.

We performed a Fortran code based on the fourth-order Runge–Kutta algorithm [16], with the initial conditions  $T_e(t=0) = T_L(t=0) = 300$  K for solving the coupled equations in TTM and computing  $T_{ws}$ .

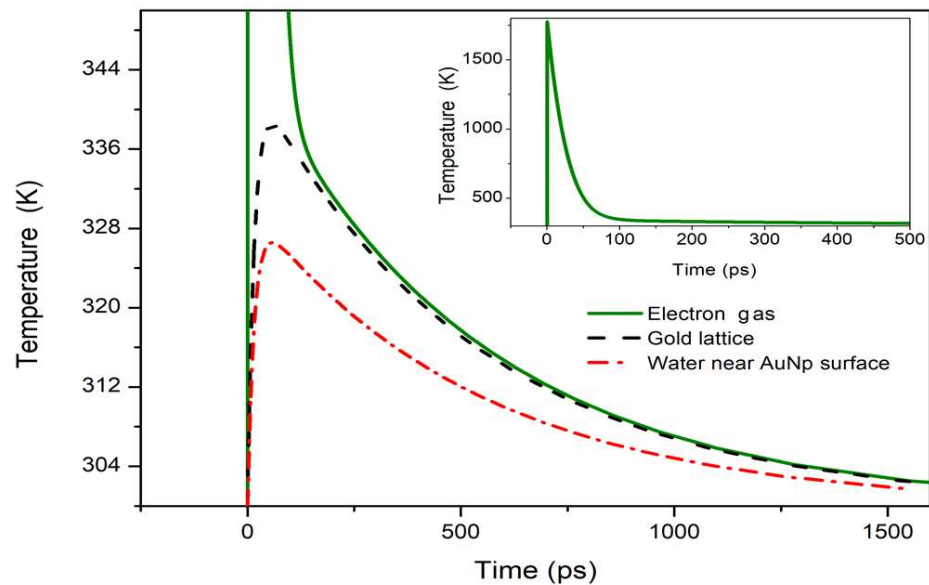
### 3. Results and Discussion

Figure 1 shows the optical cross-sections of the AuNp embedded in water. The extinction, the absorption, and the scattering as a function of wavelength were computed using Mie Code. As seen at LSPR  $\lambda = 524$  nm, the high absorption cross-section ( $C_{abs} = 3623.83$  nm<sup>2</sup>) is reported as well as weak scattering.



**Figure 1.** Optical cross-sections upon wavelengths of incident light calculated using Mie theory for the 40 nm diameter AuNp embedded in water.

We report, in Figure 2, the thermal response of the electron gas, the gold lattice, and the water near the AuNp surface when a 40 nm diameter AuNp is heated by one single femtosecond pulse laser ( $N = 1$  in Equation (3)) and cooled in water; the pulse duration is  $\tau_p = 100$  fs and the laser fluence is  $F = 1$  J/m<sup>2</sup>. The step time in the simulation is  $10^{-2}$  ps. This figure illustrates clearly the ultra-fast process of electrons compared to phonons. The temperature  $T_e$  increases to reach a temperature of 1800 K at 300 fs. The electronic thermal relaxation causes an increase in  $T_L = 340$  K at approximately 50 ps. As  $T_L$  increases, the temperature jumps at the interface; due to the heat loss from the particle surface to the water, the temperature  $T_{ws}$  of the latter begins to increase to reach its maximum value  $T_{ws} = 326$  K. The cooling time of the AuNp in the water is on average 3 ns.



**Figure 2.** Temporal evolution of  $T_e$ ,  $T_L$  and  $T_{ws}$  of 40 nm diameter AuNp heated by one single femtosecond pulse and cooled in water.  $\tau_p = 100$  fs and  $F = 1$  J/m<sup>2</sup>. In inset, temporal evolution of electron temperature.

Figure 3 shows the temporal evolution of the temperatures  $T_e$ ,  $T_L$  and  $T_{ws}$  during the irradiation by  $N = 5$  sub-pulses at  $1 \text{ J/m}^2$ ; in Figure 3a, the separation time between sub-pulses is fixed to  $t_{sep} = 2 \text{ ns}$  (0.5 GHz), which is much longer than the electron relaxation time, which is smaller than 1 ps, and the electron–phonon coupling time which is on average 50 ps, as reported in [12]. The thermal relaxation of AuNp occurs before the next sub-pulse comes. The effect of the multi-pulses on the heat accumulation is not particularly observable, since for the second sub-pulse there is only an increase of 1 K in  $T_L$  and 0.5 K in  $T_{ws}$ , with no effect for the next sub-pulses. Our conclusion is similar to that of Lutfellin et al. [5] where no heat accumulation was observed for the laser having  $\tau_p = 10 \text{ ns}$  and  $t_{sep} = 10 \text{ ns}$ . Ekici et al. [11] studied the heating of a gold nanorod irradiated with 80 pulses of  $\tau_p = 280 \text{ fs}$  and  $t_{sep} = 12.5 \text{ ns}$ ; they found that the accumulation effect is not pronounced with a temperature rise of 3 K for the first few pulses.

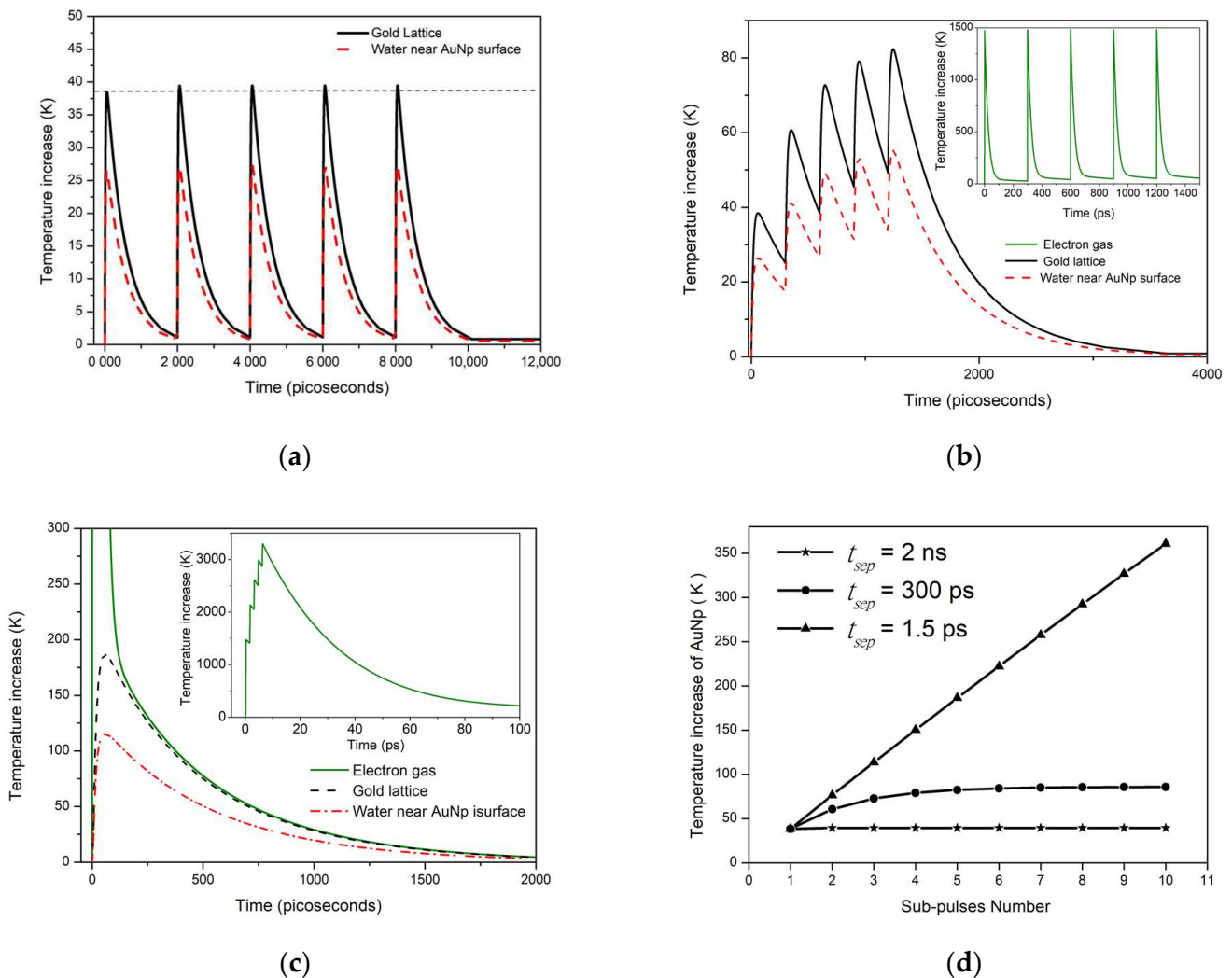


**Figure 3.** Temperature increase for 5 sub-pulses with a duration time 100 fs and a fluence of  $1 \text{ J/m}^2$ . Separation time between sub-pulses is of (a) 2 ns, (b) 300 ps and (c) 1.5 ps. The curves in (d) depict the increment of maximal temperature of AuNp as a function of the number of sub-pulses for the different separation times.

Figure 3b reports the results for  $t_{sep} = 300 \text{ ps}$  (1/3 Mhz). The repetition rate is fixed much longer than the time of the electrons’ relaxation, which occurs before the coming of the next sub-pulse; this is why in the Figure 3b inset, the maximum of  $T_e$  seems the same. The thermal accumulation is observed in the lattice and the AuNp/water interface, with a maximal temperature of  $T_L = 85 \text{ K}$  (rate of increase of 17 K/sub-pulse) and  $T_{ws} = 55 \text{ K}$

(5.5 K/sub-pulse). Ali et al., in Ref. [15], resolved the TTM in addition to the heat diffusion equation for hollow gold nanoshells irradiated with  $N = 5$  sub-pulses of  $\tau_p = 5$  ns and separated by 21 ns; they noticed a temperature rise of 0.5 K/sub-pulse because the separation time was smaller than the total relaxation time of the AuNp.

In Figure 3c,  $t_{sep} = 1.5$  ps (2/3 Mhz), which is much less than the transfer time of the thermal energy to the lattice. Fast thermal accumulation was observed, where the electrons had sufficient time to accumulate all the energy and transfer it once to the phonons and the environment, respectively. The increase in the maximal temperature of  $T_L = 190$  K (38 K/sub-pulse) and  $T_{ws} = 110$  K (22 K/sub-pulse). The curves in Figure 3d indicate the threshold sub-pulses to avoid the melting point ( $T_m$ ) of AuNp, the boiling temperature ( $T_b$ ), the critical temperature ( $T_{Cr}$ ), and the cavitation threshold of water ( $T_{cav}$ ).

#### 4. Conclusions

In this work, we investigated the energy exchange dynamics in the spherical AuNp heated by a femtosecond laser burst for several separation times between sub-pulses. The results found show that a sequence of sub-pulses, adequately separated by a time less than the thermal relaxation, is sufficient to produce fast heat accumulation, increasing the AuNp temperature as well the external temperature near the interface, without having to increase the laser energy. This accumulation process could be a good way to control the heat needed to damage cancer cells.

**Author Contributions:** Conceptualization, S.M.; methodology, S.M.; software, A.R.S.; validation, A.R.S.; formal analysis, S.M. and A.R.S.; investigation, S.M.; resources, S.M.; writing—original draft preparation, S.M.; writing—review and editing, A.R.S.; visualization, A.R.S.; supervision, A.R.S.; project administration, A.R.S. All authors have read and agreed to the published version of the manuscript.

**Funding:** This research received no external funding.

**Institutional Review Board Statement:** Not applicable.

**Informed Consent Statement:** Not applicable.

**Data Availability Statement:** Not applicable.

**Conflicts of Interest:** The authors declare no conflict of interest.

#### References

1. Rout, A.; Boltaev, G.S.; Ganeev, R.A.; Fu, Y.; Maurya, S.K.; Kim, V.V.; Rao, K.S.; Guo, C. Nonlinear Optical Studies of Gold Nanoparticle Films. *Nanomaterials* **2019**, *9*, 291. [[CrossRef](#)] [[PubMed](#)]
2. Zhang, H.; Chen, H.J.; Du, X.; Wen, D. Photothermal conversion characteristics of gold nanoparticle dispersions. *Sol. Energy* **2014**, *100*, 141–147. [[CrossRef](#)]
3. Chang, C.C.; Chen, C.P.; Wu, T.H.; Yang, C.H.; Chii-Wann Lin, C.W.; Chen, C.Y. Gold Nanoparticle-Based Colorimetric Strategies for Chemical and Biological Sensing Applications. *Nanomaterials* **2019**, *9*, 861. [[CrossRef](#)] [[PubMed](#)]
4. Amina, S.J.; Guo, B. A Review on the Synthesis and Functionalization of Gold Nanoparticles as a Drug Delivery Vehicle. *Int. J. Nanomed.* **2020**, *15*, 9823–9857. [[CrossRef](#)] [[PubMed](#)]
5. Letfullin, R.R.; Iversen, C.B.; George, T.F. Modeling nanophotothermal therapy: Kinetics of thermal ablation of healthy and cancerous cell organelles and gold nanoparticles. *Nanomed. Nanotechnol. Biol. Med.* **2011**, *7*, 137–145. [[CrossRef](#)] [[PubMed](#)]
6. Bohren, C.F.; Huffman, D.R. *Absorption and Scattering of Light by Small Particles*; Wiley-Interscience: New York, NY, USA, 1983.
7. Wrigglesworth, E.G.; Johnston, J.H. Mie theory and the dichroic effect for spherical gold nanoparticles: An experimental approach. *Nanoscale Adv.* **2021**, *3*, 3530–3536. [[CrossRef](#)] [[PubMed](#)]
8. Draine, B.T.; Flatau, P.J. User guide for the discrete dipole approximation code DDSCAT 7.3. *arXiv* **2013**, arXiv:1002.1505.
9. Anisimov, I.S.; Kapeliovich, B.L.; Perel'man, T.L. Electron emission from metal surfaces exposed to ultrashort laser pulses. *Sov. Phys. JETP* **1974**, *39*, 375–377.
10. Majchrzak, E.; Dziatkiewicz, J. Analysis of ultra-short laser pulse interactions with metal films, using a two-temperature model. *J. Appl. Math. Comput. Mech.* **2015**, *14*, 31–39. [[CrossRef](#)]
11. Ekici, O.; Harrison, R.K.; Durr, N.J.; Eversole, D.S.; Lee, M.; Ben-Yakar, A. Thermal analysis of gold nanorods heated with femtosecond laser pulses. *J. Phys. D Appl. Phys.* **2008**, *4*, 185501. [[CrossRef](#)] [[PubMed](#)]

12. Gan, R.; Fan, H.; Wei, Z.; Liu, H.; Lan, S.; Dai, Q. Photothermal Response of Hollow Gold Nanorods under Femtosecond Laser Irradiation. *Nanomaterials* **2019**, *9*, 711. [[CrossRef](#)] [[PubMed](#)]
13. Pustovalov, K.V. Theoretical study of heating of spherical nanoparticle in media by short laser pulses. *Chem. Phys.* **2005**, *308*, 103–108. [[CrossRef](#)]
14. Volkov, A.N.; Sevilla, C.; Zhigilei, L.V. Numerical modeling of short pulse laser interaction with Au nanoparticle surrounded by water. *Appl. Surf. Sci.* **2007**, *253*, 6394–6399. [[CrossRef](#)]
15. Ali, H.; Simon, F.D.; Michel, M. Simulation of nanosecond laser-induced thermal dynamics of hollow gold nanoshells for hyperthermia therapy. *AIP Conf. Proc.* **2014**, *1590*, 105.
16. Carpenter, M.; Kennedy, C.A. *Fourth-Order 2N-Storage Runge-Kutta Schemes*; NASA: Washington, DC, USA, 1994; p. 24.

**Disclaimer/Publisher's Note:** The statements, opinions and data contained in all publications are solely those of the individual author(s) and contributor(s) and not of MDPI and/or the editor(s). MDPI and/or the editor(s) disclaim responsibility for any injury to people or property resulting from any ideas, methods, instructions or products referred to in the content.